MATHEMATICS OF COMPUTATION, VOLUME 27, NUMBER 124, OCTOBER 1973

Eigenfrequencies of an Elliptic Membrane*

By B. A. Troesch and H. R. Troesch

Abstract. The first few eigenfrequencies of a homogeneous elliptic membrane, which is fixed along its boundary, are given in a graph. It is explained in detail, how more accurate results can readily be obtained for special purposes. The known expansion of the eigenfrequencies for small and large eccentricities are summarized. As an application some nodal patterns for a membrane with a double eigenvalue are presented.

1. Introduction. The free vibrations of elliptic membranes and related problems have been investigated extensively since E. Mathieu's work a hundred years ago ([7], [1] and [3, p. 525], and the references given there). The determination of the eigenfrequencies of an elliptic membrane, which is fixed along its boundary, leads to the problem of finding the roots of the radial (or modified) Mathieu functions. Although these functions have been tabulated in part ([5], [6], [14]), the membrane frequencies, especially for the higher modes, are apparently not available in easily accessible form [15].

It is the purpose of this paper to fill this gap and to present in simple form (see Fig. 1) the fundamental and a few higher harmonic frequencies for elliptic membranes as a function of the eccentricity. When dealing with Mathieu functions, it is often difficult to extract the necessary information quickly from the available literature, especially from more than one source, since the notation and the normalization have not yet been standardized. For this reason, we present the results in such a way that only reference [1] is actually needed. (The only exceptions are the formulas from [8] and [9], which are used for the expansions in Sections 5 and 6.) The use of Fig. 1 is facilitated by the sketch of the corresponding nodal patterns and the limiting eigenvalues given in Table 1. Quite on purpose, no scaling of any kind has been introduced.

The summary of the mathematical background (including the notation) is presented in Section 2, following mainly [2]. For the cases where the Fig. 1 does not furnish results of sufficient accuracy, the computational method to improve the precision is explained in Section 3, and some further details are given in connection with Problem 2 in Section 4.

2. Problem Statement and Notation. The harmonic vibrations of a homogeneous membrane are governed by the reduced wave equation for the small deflection φ:

$$\nabla^2\varphi + \lambda\varphi = 0; \tag{2.1}$$

Received September 6, 1972.

AMS (MOS) subject classifications (1970). Primary 35J05, 73K15; Secondary 35J25, 70J10, 33A55.

Key words and phrases. Linear membrane vibrations, Mathieu functions, Helmholtz equation in elliptic coordinates.

* This work was supported by the National Science Foundation grant GP-22587.

Copyright © 1973, American Mathematical Society

License or copyright restrictions may apply to redistribution; see https://www.ams.org/journal-terms-of-use

and, if the membrane is fixed along its boundary, φ is subject to the boundary condition

$$\varphi = 0. \tag{2.2}$$

The eigenvalues $\lambda = \rho\omega^2/T$ depend on the frequency of the free vibration ω, the density ρ, and the tension T.

For elliptic membranes, elliptic coordinates ξ, η are introduced; they are related to the cartesian coordinates x', y' by

$$\begin{aligned} x' &= c \cosh \xi \cos \eta, \\ y' &= c \sinh \xi \sin \eta, \end{aligned} \qquad 0 \leqq \xi < \infty, 0 \leqq \eta < 2\pi. \tag{2.3}$$

The curves ξ = constant are confocal ellipses with the focal points at $x' = \pm c$. (The dashed quantities for the cartesian coordinates are used here to avoid a possible conflict with the meaning of x and y in [1].)

In elliptic coordinates, Eq. (2.1) becomes

$$\varphi_{\xi\xi} + \varphi_{\eta\eta} + (\lambda c^2/2)(\cosh 2\xi - \cos 2\eta)\varphi = 0,$$

and separation of variables $\varphi = X(\xi)Y(\eta)$ leads to the Mathieu differential equation

$$Y'' + (a^* - 2q \cos 2\eta)\, Y = 0 \tag{2.4}$$

(cf. [1, Eq. (2.01)]) and to the modified Mathieu differential equation

$$X'' - (a^* - 2q \cosh 2\xi)X = 0. \tag{2.5}$$

Here, a^* denotes the separation constant and

$$4q = \lambda c^2. \tag{2.6}$$

The alternate notation in [1] will also be used, namely

$$s = \lambda c^2, \tag{2.7}$$

and we note in passing that this important parameter s is called $4k^2$ in [8] and $4h^2$ in [9].

The solutions of Eq. (2.4) which are appropriate for our problem must be periodic with period π or 2π, and are called

$$ce_m(\eta, q) \quad \text{and} \quad se_{m+1}(\eta, q), \qquad m = 0, 1, 2, \cdots. \tag{2.8}$$

Together with the solutions of the modified Mathieu equation (2.5), the solutions of Eq. (2.1) then become

$$\varphi = Ce_m(\xi, q)ce_m(\eta, q) \tag{2.9}$$

and

$$\varphi = Se_{m+1}(\xi, q)se_{m+1}(\eta, q) \tag{2.10}$$

for $m = 0, 1, 2, \cdots$.

If the boundary of the elliptical membrane corresponds to $\xi = \xi_0$, its equation is (cf. Eq. (2.3))

$$\frac{x'^2}{c^2 \cosh^2 \xi_0} + \frac{y'^2}{c^2 \sinh^2 \xi_0} = 1$$

License or copyright restrictions may apply to redistribution; see https://www.ams.org/journal-terms-of-use

with the major axis

$$a = c \cosh \xi_0, \tag{2.11}$$

the minor axis

$$b = c \sinh \xi_0, \tag{2.12}$$

and

$$c^2 = a^2 - b^2. \tag{2.13}$$

3. The Method of Computation. In this section, the method of finding the eigenfrequencies of an elliptic membrane will be outlined. Further details are explained in connection with the Problem 2 below.

If we wish to find the eigenvalues λ for one fixed ellipse with axes a and b (c and ξ_0 are then determined by Eqs. (2.11) to (2.13)), we must compute all q values (see Eq. (2.6)) for which the modified, or radial, Mathieu functions $Ce_m(\xi_0, q)$ or $Se_{m+1}(\xi_0, q)$ vanish. In order to obtain the results needed in Fig. 1, it is, however, much simpler to reverse the process and to find the roots ξ_0 of Ce_m and Se_{m+1} for a given q (or, equivalently, a given s), since [1] then furnishes the basic information just in the proper form. The functions

$$Je_r(s, x) \quad \text{and} \quad Jo_r(s, x), \tag{3.1}$$

introduced in [1], where

$$x = \xi, \tag{3.2}$$

are proportional to Ce_r and Se_r [1, p. xxxviii]. The roots are best found by using Eqs. (3.03) and (3.04) (cf. the remark on p. xxi), or for our purpose simply

$$\sum_{k=0}^{\infty} (-1)^k De_{2k+p} J_{2k+p}(s^{1/2} \cosh x) = 0, \tag{3.3}$$

$$\sum_{k=0}^{\infty} (-1)^k (2k + p) Do_{2k+p} J_{2k+p}(s^{1/2} \cosh x) = 0, \tag{3.4}$$

where $p = 0$, 1, and J are the Bessel functions. Since the coefficients De and Do are tabulated in [1] for different values of r, we need not be concerned with the separation constant a^*. Furthermore, the different normalizations appearing in the literature for the radial Mathieu functions can also be ignored for the determination of the root ξ_0.

From the roots $s^{1/2} \cosh \xi_0$ (now returning to our notation), we find, from Eqs. (2.7) and (2.11),

$$\lambda^{1/2} a = s^{1/2} \cosh \xi_0 \tag{3.5}$$

and

$$\lambda^{1/2} b = s^{1/2} \sinh \xi_0 = (\lambda a^2 - s)^{1/2}. \tag{3.6}$$

It turns out that this last quantity is well suited for plotting the results as a function of the independent variable

License or copyright restrictions may apply to redistribution; see https://www.ams.org/journal-terms-of-use

$$(1 - e^2)^{1/2} = b/a, \tag{3.7}$$

since the $\lambda^{1/2}b$ curves stay finite and have finite slope at the limiting eccentricities $e = c/a$, i.e., at $e = 0$ and $e = 1$. Then Fig. 1 gives the eigenvalues for ellipses with axes a and b which fall within a certain range. If ellipses with a fixed area A are to be compared, then we note that

$$\lambda = \frac{\pi}{A} \frac{(\lambda^{1/2}b)^2}{(1 - e^2)^{1/2}}, \tag{3.8}$$

so that λ is constant on parabolas through $\lambda^{1/2}b = 0$, $e = 1$, opening to the left.

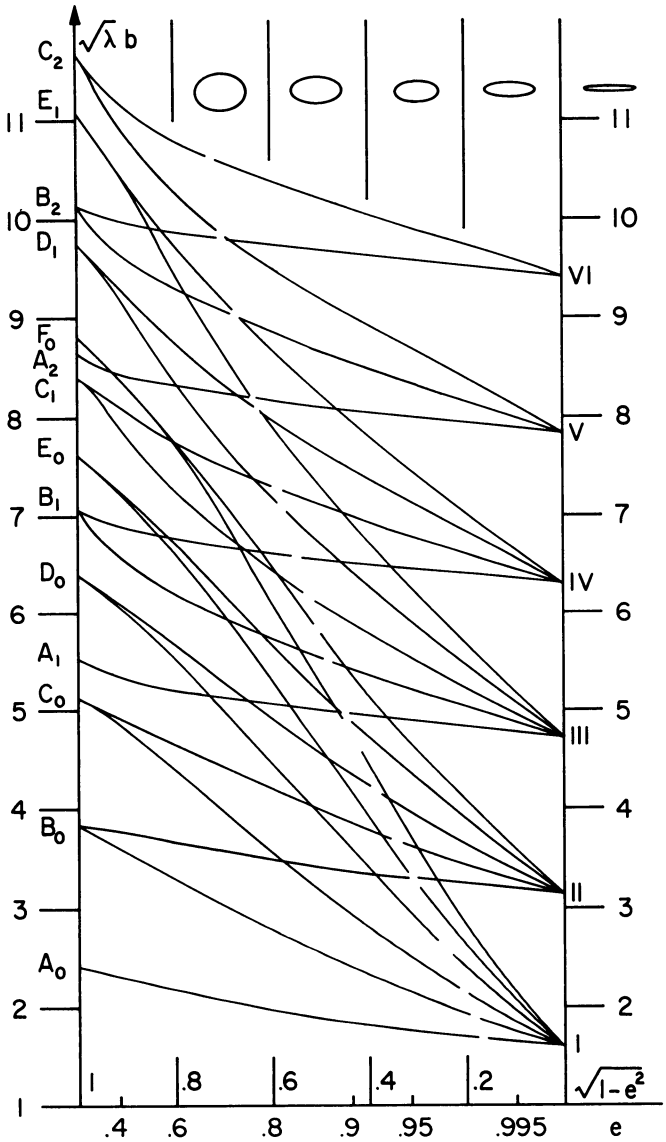

FIGURE 1. *The lowest eigenfrequencies of a fixed membrane*

License or copyright restrictions may apply to redistribution; see https://www.ams.org/journal-terms-of-use

TABLE 1. *Nodal patterns and limits of eigenvalues*

Point	$\lambda^{1/2}b$	Mathieu function	Nodal pattern
Point I, $\lambda^{1/2}b = \pi/2$			
F_0	8.7715	Ce_5	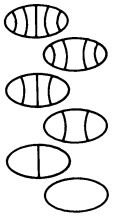
E_0	7.5883	Ce_4	
D_0	6.3802	Ce_3	
C_0	5.1356	Ce_2	
B_0	3.8317	Ce_1	
A_0	2.4048	Ce_0	
Point II, $\lambda^{1/2}b = \pi$			
		Se_5	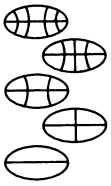
		Se_4	
		Se_3	
		Se_2	
		Se_1	
Point III, $\lambda^{1/2}b = 3\pi/2$			
E_1	11.0647	Ce_4	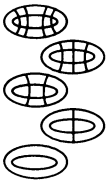
D_1	9.7610	Ce_3	
C_1	8.4172	Ce_2	
B_1	7.0156	Ce_1	
A_1	5.5201	Ce_0	
Point IV, $\lambda^{1/2}b = 2\pi$			
		Se_4	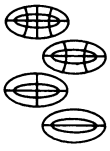
		Se_3	
		Se_2	
		Se_1	
Point V, $\lambda^{1/2}b = 5\pi/2$			
C_2	11.6198	Ce_2	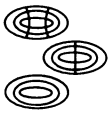
B_2	10.1735	Ce_1	
A_2	8.6537	Ce_0	
Point VI, $\lambda^{1/2}b = 3\pi$			
		Se_2	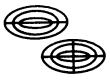
		Se_1	

Returning now to the problem of finding the roots of Eqs. (3.3) and (3.4), we observe that the well-known recursive computation of the Bessel functions [12] is very well suited for our purpose. We need the relation

$$J_{n-1}(s^{1/2}\cosh\xi) = \frac{2n}{s^{1/2}\cosh\xi}\,J_n(s^{1/2}\cosh\xi) - J_{n+1}(s^{1/2}\cosh\xi),$$

and for the root-finding by Newton's method

$$J_n'(s^{1/2}\cosh\xi) = \frac{n}{s^{1/2}\cosh\xi}\,J_n(s^{1/2}\cosh\xi) - J_{n+1}(s^{1/2}\cosh\xi).$$

Further details will be explained in Problem 2 in the next section.

4. Applications. For the first two problems to be considered, we choose an elliptical membrane and compare the following two modes:

License or copyright restrictions may apply to redistribution; see https://www.ams.org/journal-terms-of-use

(a) The mode without a nodal line along the major axis (this leads to the solutions Eq. (2.9)), but with three hyperbolas as nodal lines. In Table 1, we find this pattern under (D_0, I) with the corresponding curve in Fig. 1.

(b) The mode without a nodal line along the major axis and one elliptical nodal line, but no hyperbolas. In Table 1, this pattern is (A_1, III).

Problem 1. For the ellipse with major axis $a = 4$ and minor axis $b = 3$, which of the two nodal patterns, (a) and (b) above, has the lower eigenvalue λ, and what is its approximate value?

Solution. We have $b/a = (1 - e^2)^{1/2} = 3/4$.

From Fig. 1, we conclude immediately, that the mode (A_1, III) represents the solution, since this curve lies slightly below the curve (D_0, I). We also read off that $\lambda^{1/2}b \doteq 5.25$, and hence $\lambda \doteq 3.06$.

Problem 2. Find the eccentricity e for which the eigenvalues of the two nodal patterns above are the same, and determine some nontrivial nodal patterns (cf. Figs. 2 to 4).

Remark. For simple eigenvalues, it is obvious that all nodal lines in an elliptic membrane must be (nondegenerate or degenerate) confocal ellipses and hyperbolas. For a multiple eigenvalue, any linear combination of solutions of Eq. (2.1) is again a solution, and this gives rise to special nodal patterns. Fig. 1 shows that there is an abundance of multiple eigenvalues for ellipses. This is in contrast to the circular membrane where there exist no multiple eigenvalues except for the obvious double eigenvalues. (For a proof of this statement, see [13, p. 484].) Therefore, the nodal lines in circular membranes are without exception circular or straight lines.

Solution. Let us assume here that the eccentricity and the eigenvalue λ are required to greater accuracy than can be obtained from Fig. 1. The necessary steps in the computation are then:

(1) Fig. 2 shows that the curves (D_0, I) and (A_1, III) intersect near

$$(1 - e^2)^{1/2} \doteq .73 \quad \text{and} \quad \lambda^{1/2}b = 5.15.$$

(2) The approximate value of s then becomes (cf. Eqs. (2.11), (2.13), (3.7))

$$s = e^2(1 - e^2)^{-1}\lambda b^2 \doteq 23.3. \tag{4.1}$$

This value is not very accurate, as we will see below (s is rather sensitive to errors in the eccentricity), but still more than adequate for the following step.

(3) Next, we compute the roots of Ce_0 and Ce_3 (or Je_0 and Je_3 in the notation of [1]) for s values around the approximate s, and this is carried out for $s = 21, 22, 23, 24, 25$, by using Eq. (3.3).

The coefficients are found in [1], on p. 48 for Ce_0, and on p. 93 for Ce_3. The approximate argument in the Bessel function is (cf. Eqs. (3.5), (3.7))

$$s^{1/2} \cosh \xi_0 = \lambda^{1/2}a = \lambda^{1/2}b(1 - e^2)^{-1/2} \doteq 7.05.$$

Newton's method applied to Eq. (3.3) gives the values of $\lambda^{1/2}a$ in two to three iterations, and, for the set of s values above, the roots turn out to be between 6.9 and 7.2. From Eq. (3.6), we obtain

$$\lambda^{1/2}b = (s \cosh^2 \xi_0 - s)^{1/2},$$

and these values are listed in Table 2.

License or copyright restrictions may apply to redistribution; see https://www.ams.org/journal-terms-of-use

TABLE 2. *Values of* $\lambda^{1/2}b$ *for the modes* (a) *and* (b)

s	$\lambda^{1/2}b$ for $Ce_0 = 0$	$\lambda^{1/2}b$ for $Ce_3 = 0$
21	5.167083	5.285691
22	5.160278	5.221560
23	5.153762	5.157058
24	5.147514	5.092291
25	5.141516	5.027364

(4) The intersection of the two $\lambda^{1/2}b$ curves is found to be at

$$4q_0 = s_0 = 23.05654, \qquad \lambda^{1/2}b = 5.153402$$

and the remaining quantities follow easily:

$$\lambda^{1/2}a = 7.043727, \qquad \xi_0 = .932226,$$

$$b/a = (1 - e^2)^{1/2} = .7316300, \qquad e = .6817019.$$

(5) In order to find the nodal patterns shown in Figs. 2, 3, and 4, we need the four functions $Ce_0(\xi, q_0)$, $Ce_3(\xi, q_0)$, $ce_0(\eta, q_0)$, $ce_3(\eta, q_0)$ or, since the amplitudes are irrelevant, solutions proportional to them. The coefficients De for Ce_0 and Ce_3 are interpolated from [1] for the s_0 given above, and the left-hand side of Eq. (3.3) computed for $0 \leqq \xi \leqq \xi_0$. The computation of the functions $ce_0(\eta, q_0)$, $ce_3(\eta, q_0)$ uses the same coefficients (cf. [1, Eqs. (1.6), (1.7)])

$$ce_0(\eta, q) = \sum_{k=0}^{\infty} De_{2k} \cos 2k\eta, \qquad ce_3(\eta, q) = \sum_{k=0}^{\infty} De_{2k+1} \cos(2k + 1)\eta.$$

If we now write the solution of Eq. (2.1) as

$$\varphi = Kce_3(\eta, q_0)Ce_3(\xi, q_0) + ce_0(\eta, q_0)Ce_0(\xi, q_0),$$

and find for the assumed constant K the roots $\varphi = 0$, we obtain the nodal lines. The three special patterns in Figs. 2, 3, and 4 are readily found by varying K and observing the effect. The six points obtained from the intersections of the nodal lines in the modes (a) and (b) do not change with K. The plotting is best carried out by using Eq. (2.3).

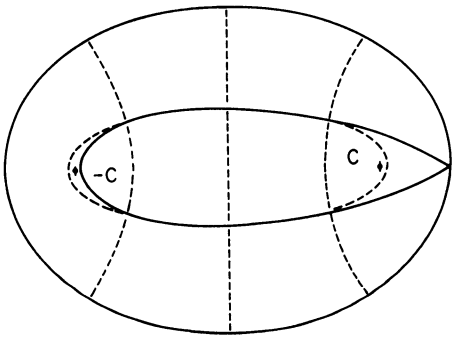

FIGURE 2. *Example of a nodal pattern for Problem* 2

License or copyright restrictions may apply to redistribution; see https://www.ams.org/journal-terms-of-use

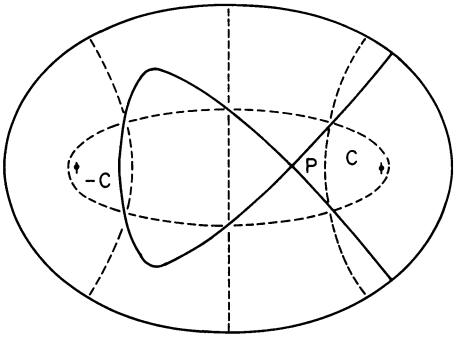

FIGURE 3. *Example of a nodal pattern for Problem* 2

It can be shown that the special points P in Figs. 3 and 4 occur at

$$\eta = \eta_0 \doteq 1.16 \quad \text{and} \quad \eta = \pi - \eta_0,$$

where η_0 is the solution of

$$ce_0(\eta_0)ce_3'(\eta_0) - ce_0'(\eta_0)ce_3(\eta_0) = 0.$$

Problem 3. Find the fundamental eigenvalue λ for the ellipse with $b = a/2$.

Solution. The fundamental eigenvalue belongs to the root of Ce_0 or the curve (A_0, I) in Fig. 1. For $e = 3^{1/2}/2$ or $(1 - e^2)^{1/2} = \frac{1}{2}$ we read off

$$\lambda^{1/2}b \doteq 1.9,$$

hence (cf. Eq. (4.1))

$$s = 3(\lambda^{1/2}b)^2 \doteq 10.8,$$

and, proceeding as above, the results in Table 3 are obtained.

The result

$$\lambda^{1/2}a = 3.77715 \pm 1 \cdot 10^{-5}$$

for $e = 3^{1/2}/2$ furnishes the answer to the open entry in [10, p. 6].

5. Expansion for Small Eccentricity. For nearly circular membranes, the table of coefficients in [1] makes it easy to find the eigenvalues by the general method

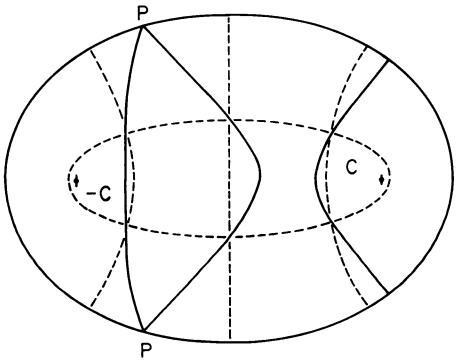

FIGURE 4. *Example of a nodal pattern for Problem* 2

License or copyright restrictions may apply to redistribution; see https://www.ams.org/journal-terms-of-use

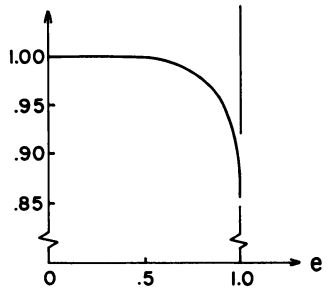

FIGURE 5. $\lambda(1/a^2 + 1/b^2)^{-1}$ *for the fundamental eigenvalue of ellipses*

described above. But it is still desirable to have an expansion of the eigenvalues for small eccentricity. As it turns out, the trend of the eigenvalues at $e = 0$ can be described very simply, particularly in the variables $\lambda^{1/2}b$ and $e^* = 1 - (1 - e^2)^{1/2}$ used in Fig. 1:

(a) the slope of all the curves is negative; all the tangents meet at the same point on the e^*-axis, except for Ce_1 and Se_1;

(b) the curvature of all the curves is negative, except for Ce_0, Ce_1, Se_1, Se_2, where the curvature is always positive;

(c) for $m = 0$ and $m \geqq 3$ the curves for Ce_m and Se_m agree in the first three terms (see Eq. (5.1) below). Therefore, more terms would be needed for eccentricities for which Ce_m and Se_m are observed to differ in Fig. 1.

The expansion for small eccentricity is given in [9, Section 2.85, Eqs. (9) and (10)], and reads (in our notation)

$$s^{1/2} \cosh \xi_0 = \lambda^{1/2}a = u_k + c_1 s/u_k + c_2 s^2/u_k^2 + O(s^3) \tag{5.1}$$

for the kth eigenvalue of the radial Mathieu functions Ce_m and Se_m. The constants c_1 and c_2 are listed in [9], and u_k denotes the kth positive root of the Bessel function $J_m(u_k)$. For $m = 1$ and $m = 2$ the constant c_2 depends on u_k. It is rather straightforward to write Eq. (5.1) in terms of $\lambda^{1/2}b$ and e^*. From this form of the result, the trends described above then become obvious. An expansion of the fundamental eigenvalue to even higher terms is given in [4].

6. Expansion for Large Eccentricity. Since the values of the coefficients De and Do in [1] do not extend beyond $s = 100$ (cf. the gaps in Fig. 1), the connection to $e = 1$ (i.e., $s = \infty$) is best accomplished by an expansion. Indeed, the expansion below

TABLE 3. *Fundamental* $\lambda^{1/2}a$ *for an elliptic membrane with* $b = a/2$

s	e	$\lambda^{1/2}a$
9.5	.849864	3.626708
10.0	.857016	3.689871
10.5	.863560	3.752341
11.0	.869566	3.814114
11.5	.875096	3.875192

License or copyright restrictions may apply to redistribution; see https://www.ams.org/journal-terms-of-use

gives accurate results for $s = 100$, except for Ce_4, Se_4, and Ce_5, where the error is between 1% and 2%. But even then, it is easy to connect the expansion smoothly with the numerically computed curves.

The expansions of the roots of the modified Mathieu functions for large eccentricity are known. As a starting point, we choose the formulas in [8, p. 385] (cf. also [9, p. 211, p. 213], [11, p. 8]) which read in our notation

$$\left(1 + \frac{2m+1}{4s^{1/2}\cosh^2\xi_0}\right)\begin{Bmatrix}\cos\\ \sin\end{Bmatrix}\left(s^{1/2}\sinh\xi_0 - \frac{2m+1}{2}\tan^{-1}\sinh\xi_0\right)$$
$$- \frac{m^2+m+1}{4s\cosh^2\xi_0}\,s^{1/2}\sinh\xi_0\begin{Bmatrix}\sin\\ \cos\end{Bmatrix}\left(\frac{2m+1}{2}\tan^{-1}\sinh\xi_0 - s^{1/2}\sinh\xi_0\right) = 0,$$

where the upper alternative is valid for Ce_m, the lower alternative for Se_{m+1}. A reasonably straightforward transformation to an expansion for the kth root in terms of $(1-e^2)^{1/2}$ leads then to

$$\lambda^{1/2}b = s^{1/2}\sinh\xi_k = (k+\tfrac{1}{2})\pi + (m+\tfrac{1}{2})(1-e^2)^{1/2} + \frac{m^2+m+1}{(4k+2)\pi}(1-e^2) + O((1-e^2)^{3/2})$$

for $Ce_m(\xi_k, q)$, and

$$\lambda^{1/2}b = s^{1/2}\sinh\xi_k = k\pi + (m+\tfrac{1}{2})(1-e^2)^{1/2} + \frac{m^2+m+1}{4k\pi}(1-e^2) + O((1-e^2)^{3/2})$$

for $Se_{m+1}(\xi_k, q)$.

Appendices.

A. *A Numerical Approximation for the Two Lowest Eigenvalues.* It is sometimes convenient to have an approximate formula available for use on a computer. We give here possible polynomial approximations for the two lowest modes in terms of $e^* = 1 - (1-e^2)^{1/2}$:

$$\lambda^{1/2}b = \sum_{k=0}^{5}\alpha_k(e^*)^k,$$

where the coefficients are listed in Table 4.

These approximations are correct at the endpoints and have a maximum relative error of about $2\cdot 10^{-4}$.

B. *Combinations of Dimensionless Quantities.* In [10], G. Pólya and G. Szegö list on pp. 265–270 dimensionless combinations involving the fundamental eigenvalue

TABLE 4. *A polynomial approximation*

Coefficients for	α_0	α_1	α_2	α_3	α_4	α_5
fundamental mode	2.4048	−1.1924	.1768	.3923	−.2107	0
first harmonic	3.8317	−2.8826	.3897	−.2749	1.1417	−.6348

License or copyright restrictions may apply to redistribution; see https://www.ams.org/journal-terms-of-use

λ of a membrane. We have evaluated these combinations numerically, and also the combinations multiplied by b/a, where this factor is required to keep the limit $e \to 1$ bounded. Without exception, the particular combinations change monotonically with the eccentricity of the elliptical membrane, and it can be safely conjectured that this is indeed the case mathematically. But there exist, of course, less natural dimensionless expressions where monotonicity no longer holds.

Incidentally, one of the combinations is somewhat remarkable in that it stays within $\frac{1}{2}\%$ of the value for the circle up to an eccentricity as large as $e = .65$ (see Fig. 5). It is the dimensionless quantity $\lambda A/B$, or, in the case of ellipses,

$$\lambda(1/a^2 + 1/b^2)^{-1}. \tag{B.1}$$

This observation may, however, not be so surprising, if we note [10, p. 99] that the expression (B.1) is constant for rectangles of any shape.

Acknowledgment. The authors wish to express their gratitude to E. Isaacson and G. Logemann for many stimulating discussions. Their work on the eigenvalues of elliptic membranes led to our interest in this question and to the present investigation.

Department of Mathematics
University of Southern California
Los Angeles, California 90007

1. *Tables Relating to Mathieu Functions*, Nat. Bur. Standards, Appl. Math. Ser., vol. 59, Washington, D. C., 1967.
2. S. D. DAYMOND, "The principal frequencies of vibrating systems with elliptic boundaries," *Quart. J. Mech. Appl. Math.*, v. 8, 1955, pp. 361–372. MR **17,** 792.
3. A. FLETCHER, J. C. P. MILLER, L. ROSENHEAD & L. J. COMRIE, *An Index of Mathematical Tables.* Vol. 1: *Introduction.* Part I: *Index According to Functions,* 2nd ed., Addison-Wesley, Reading, Mass., 1962. MR **26** #365a.
4. J. G. HERRIOT, *The Principal Frequency of an Elliptic Membrane*, Department of Mathematics, Stanford University Report, 31 August 1949. Contract N6-ORI-106.
5. M. J. KING & J. C. WILTSE, *Derivatives, Zeros and Other Data Pertaining to Mathieu Functions*, Johns Hopkins University Radiation Laboratory, Techn. Report No. AF-57, Baltimore, Md., 1958.
6. E. T. KIRKPATRICK, "Tables of values of the modified Mathieu functions," *Math. Comp.*, v. 14, 1960, pp. 118–129. MR **22** #4126.
7. E. MATHIEU, "Mémoire sur le mouvement vibratoire d'une membrane de forme elliptique," *J. Math. Pures Appl.*, v. 13, 1868, pp. 137–203.
8. N. W. MCLACHLAN, *Theory and Application of Mathieu Functions*, Dover, New York, 1964. MR 30 #5001.
9. J. MEIXNER & F. W. SCHÄFKE, *Mathieusche Funktionen und Sphäroidfunktionen mit Anwendungen auf physikalische und technische Probleme,* Die Grundlehren der math. Wissenschaften in Einzeldarstellungen mit besonderer Berücksichtigung der Anwendungsgebiete, Band 71, Springer-Verlag, Berlin, 1954. MR **16,** 586.
10. G. PÓLYA & G. SZEGÖ, *Isoperimetric Inequalities in Mathematical Physics*, Ann. of Math. Studies, no. 27, Princeton Univ. Press, Princeton, N.J., 1951. MR **13,** 270.
11. M. J. DE SCHWARZ, "Determinazione delle frequenze e delle linee nodali di una membrana ellittica oscillante con contorno fisso," *Atti Accad. Sci. Fis. Mat. Napoli,* (3), v. 3, 1951, pp. 1–17.
12. I. A. STEGUN & M. ABRAMOWITZ, "Generation of Bessel functions on high speed computers," *MTAC*, v. 11, 1957, pp. 255–257. MR **20** #459.
13. G. N. WATSON, *A Treatise on the Theory of Bessel Functions*, 2nd ed., Cambridge Univ. Press, Cambridge; Macmillan, New York, 1944. MR **6,** 64.
14. J. C. WILTSE & M. J. KING, *Values of the Mathieu Functions,* Johns Hopkins University Radiation Laboratory, Techn. Report No. AF-53, Baltimore, Md., 1958.
15. J. W. WRENCH, JR., Private communication.

License or copyright restrictions may apply to redistribution; see https://www.ams.org/journal-terms-of-use